Surface & Coatings Technology 325 (2017) 52–57

Contents lists available at ScienceDirect

Surface & Coatings Technology

journal homepage: www.elsevier.com/locate/surfcoat

Superhydrophobic nanocoatings prepared by a novel vacuum cold spray process

Zhe Wang [a,b], Xiuyong Chen [a,*], Yongfeng Gong [a], Botao Zhang [a,c], Hua Li [a,*]

[a] Key Laboratory of Marine Materials and Related Technologies, Key Laboratory of Marine Materials and Protective Technologies of Zhejiang Province, Ningbo Institute of Materials Technology and Engineering, Chinese Academy of Sciences, Ningbo 315201, China
[b] University of Chinese Academy of Science, Beijing 100049, China
[c] Cixi Institute of Biomedical Engineering, Institute of Materials Technology and Engineering, Chinese Academy of Sciences, Ningbo 315201, China

ARTICLE INFO

Article history:
Received 28 March 2017
Revised 16 June 2017
Accepted in revised form 17 June 2017
Available online 19 June 2017

Keywords:
Superhydrophobicity
Nanocoating
Inorganic-organic nanocomposite
Vacuum cold spray

ABSTRACT

A superhydrophobic TiO_2-oleic acid (OA) nanocomposite coating was fabricated by a novel vacuum cold spray (VCS) process at room temperature. The content of OA immobilized on TiO_2 nanoparticles could influence the deposition effect during the VCS process, in turn controlling the wettability of nanocoatings acquired. The wettability of the nanocoatings could be adjusted by altering the content of OA in the starting nanocomposite powder. The maximum static water contact angle and the minimum sliding angle were obtained at 151.2°and 1.2°, respectively, with the molar ratio of OA to TiO_2 at 1:10. Additionally, it was observed that the newly constructed superhydrophobic coatings display mechanical durability. This study presents a promising approach for fabricating inorganic-organic nanocomposite superhydrophobic coatings for long-term functional applications.

1. Introduction

Superhydrophobic surfaces with water contact angles (CA) higher than 150°and sliding angles (SA) <10°have drawn great interests due to their potential applications such as anti-fouling [1], anti-corrosion [2], anti-icing [3], oil/water separation [4], drag-reducing [5], etc. Generally, a rough structure and low surface energy is required for fabricating a superhydrophobic surface [6]. Instead of directly constructing rough structures on target substrates, decorating substrates with extra-substrate nanostructured coatings or layers are more versatile and convenient [7]. With a combination of nanotechnology and superhydrophobic surfaces, superhydrophobic nanocoatings that contain at least one nanoscale raw material have drawn extensive attention recently [8–12].

To fabricate superhydrophobic nanocoatings, many approaches have been attempted, such as sol-gel [13], electrodeposition [14], dip-coating [15], template [16], and spraying [17]. Ming et al. developed a dual-size hierarchical structure with raspberry-like particles by grafting 70 nm silica particles to 700 nm ones and obtained a CA of 165° [18]. Using surface-functionalized SiO_2, ZnO and ITO nanoparticles, Bhushan et al. produced transparent superhydrophobic surfaces on glass, polycarbonate and poly(methyl methacrylate) (PMMA) substrates by a dip coating technique [9]. By spraying suspensions of silica nanoparticles immobilized with dodecyltrichlorosilane, Hitoshi et al. prepared a transparent superhyodrophobic nanocoating on paper [17]. Our group has been making effort toward superhydrophobic nanocoatings using a suspension thermal spray technique [19–20]. Polyurethane/nano-Al_2O_3 composite superhydrophobic coatings were prepared in large scale on arc-sprayed Al coatings by a suspension flame spray process for anti-corrosion applications [19]. And a superhydrophobic coating with mechanical robustness and easy-repairability was produced by a combined approach of plasma spray and suspension flame spray [20].

Vacuum cold spray (VCS) is known as a ceramic coating technology that deposits submicrometer-sized particles at room temperature. The most remarkable advantages of VCS are its possibility of depositing at room temperature, high deposition rate (up to tens of μm/min), and ability to deposit nanomaterials [21]. The VCS system has now been mainly used to prepare functional coatings for electrical, thermal and biomedical applications, for example TiO_2 films in dye-sensitized solar cells [22], $SrTi_{0.7}Fe_{0.3}O_{3-\delta}$ sensor films [23], and hydroxyapatite/graphene composite biomedical coatings [24]. Nevertheless, to the best of our knowledge, no study is reported that employs VCS to construct superhydrophobic nanocoatings.

Here we report for the first time the use of the VCS technique to fabricate superhydrophobic nanocoating using oleic acid (OA)-modified

* Corresponding authors.
E-mail addresses: chenxiuyong@nimte.ac.cn (X. Chen), lihua@nimte.ac.cn (H. Li).

http://dx.doi.org/10.1016/j.surfcoat.2017.06.044
0257-8972/

TiO_2 nanoparticles. We designed a series of surface-modified TiO_2 nanoparticles with different molar ratio of OA to TiO_2 and studied wetting behaviors and mechanical durability of the deposited nanocoatings.

2. Experimental setup

For the preparation of nano-TiO_2/oleic acid powder, a mixture of tetrabutyl titanate (50 mL, Aladdin Chemistry Co. Ltd., China) and anhydrous ethanol was added dropwise to a water-ethanol solution (water 150 mL, ethanol 150 mL) with vigorous stirring at room temperature for 2 h. Then a specific amount of OA (Aladdin Chemistry Co. Ltd., China) were added to the mixture and refluxed for 2 h. After cooling down to room temperature, the suspension was centrifuged and the sediment was washed with acetone and ethanol for several times. The OA treated TiO_2 particles were dried at 353 K. Powder with different molar ratio of OA to TiO_2 (1:1, 1:5, and 1:10) was prepared. Both the nano-TiO_2 and nano-TiO_2/OA powder were sprayed for coating deposition using the VCS 2000 system (developed by Xi'an Jiaotong University, China). Aluminum (Al) plates were used as the substrates in this study. The spraying parameters for the VCS process are as follows: the helium gas was employed as the carrier gas with a flow rate of 6 L/min, the scanning speed was 10 mm/s and the spray distance was 10 mm.

Microstructure of the powder and coatings was characterized by transmission electron microscopy (TEM, Tecnai F20, USA) and field emission scanning electron microscope (FESEM, Hitachi S4800, Japan). Thermogravimetric analysis (TGA, Perkin Elmer Diamond TG/DTA, USA) was carried out up to 600 °C in air atmosphere with a heating rate of 10 °C/min. The chemical compositions of the samples were further characterized by Fourier transform infrared spectroscopy (FTIR, Nicolet 6700, USA). Static water contact angle and slide angle measurements were performed using a video-based optical system (Dataphysics OCA20, Germany) and five measurements were made for each sample. Surface roughness of the coatings was measured by laser scanning confocal microscope (LSCM, Zeiss LSM700, Germany). The mechanical stability and adhesive of superhydrophobic nanocoatings were evaluated by scratch testing [25–28]. The testing was carried out using 1500 grit Al_2O_3 sandpapers as the abrasion surface.

3. Results and discussion

Fig. 1 shows the schematic illustration of the fabrication process of superhydrophobic TiO_2-OA nanocomposite coatings. TiO_2 nanoparticles were firstly synthesized through a sol-gel method [29] and then surface modified with OA to obtain TiO_2-OA nanocomposite powder. Finally, the TiO_2-OA nanocomposite powder was deposited on substrates via a VCS coating technique at room temperature.

For the sol-gel method, the size of TiO_2 nanoparticles could be easily tuned through different water: alkoxide molar ratio and increase of the ratio would decrease particle size [29]. It is worth to note that the particles acquired were amorphous since no thermal treatment was involved. TEM studies reveal that TiO_2 particles were in a quasi-spherical shape yet hardly separated. And the addition of OA resulted in no shape change on nanoparticles (Fig. 2a-2, 2b–2). SEM micrographs show that particles adopted a uniform spherical morphology with an average size of 50 nm, which was consistent with TEM images. However, agglomerated nanoparticles have a great advantage in constructing hierarchical roughness [17].

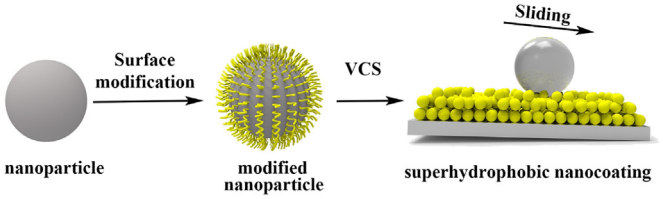

Fig. 1. Schematic illustration of the fabrication process of superhydrophobic nanocoatings.

A unique advantage of the VCS technique is that the deposition process is conducted at room temperature, ensuring the retention of organic groups. FTIR measurements were performed to confirm the retention (Fig. 3). It is shown that curve (ii) is obviously different from curve (i) but the same as curve (iii). In curve (i), the CH_2 asymmetric stretch and the symmetric stretch bands appear at 2928 and 2855 cm^{-1}, respectively. The intense peak at 1710 cm^{-1} indicates the presence of the C═O stretch, and the band at 1285 cm^{-1} is derived from the existence of C—O stretch. Two bands at 1462 and 937 cm^{-1} can be attributed to the O—H in-plane and the O—H out-of-plane stretch, respectively. In curve (ii), a little shift happen to the bands of the asymmetric CH_2 stretch and the symmetric stretch CH_2 at 2924 and 2852 cm^{-1}, respectively. The red shift indicates that the hydrocarbon chains surrounding the nanoparticles are in a close-packed, crystal state [30]. It should be noticed that the C═O stretch band of carboxyl groups, which appear at 1710 cm^{-1} in curve (i), is absent in the curve (ii). Furthermore, two brand-new peaks at 1683 and 1528 cm^{-1}, which are characteristic of the asymmetric ν_{as}(COO—) and the symmetric ν_s(COO—) stretch, dominate the spectra of OA capped TiO_2 nanoparticles. From their frequency difference, $\Delta\nu \approx 84$ cm^{-1}, the chelating bidentate mode is probably employed by carboxylate adsorbates binding onto TiO_2 surfaces [31]. These results reveal that OA is chemisorbed onto TiO_2 nanoparticles as a carboxylate and was maintained after the spray process. TGA tests further confirm the existence of OA on the coatings (Fig. 4). The little difference between curves with the same colors demonstrated that the VCS process has little effect on functionalized organic groups.

SEM photographs of coatings' surface morphology are shown in Fig. 5. For pure TiO_2 coatings (Fig. 5a–1), it shows a geometry of hills (relatively lighter region) and valleys (the darker region) in the micrometer range. A higher magnification view confirmed that the particles were densely compacted (Fig. 5a–2). For coatings with an OA: TiO_2 molar ratio of 1:1, although a certain amount of nanoparticles were deposited on to the substrate, large areas of bare Al substrate were still exposed, indicating an inappropriate deposition condition (Fig. 5b). As the content of OA decreased, the coating's coverage improved. Surfaces of coatings with an OA: TiO_2 molar ratio of 1:5 and 1:10 were similar, showing a relatively smooth geometry. At an OA: TiO_2 ratio of 1:10, coatings with a thickness of 70–80 μm were acquired, matching up to the pure TiO_2 coating. According to a previous study [22], the TiO_2 coating was deposited through a tamping effect caused by successive impact of spray particles. That is, a dense coating would be formed with successive deposition of spray particles under high impact pressure. And coatings with a porous structure would be acquired due to insufficient compaction and lack of dense aggregation between nanoparticles. Particle features especially particle size play a crucial role in the tamping effect and coating formation. Although the size of primary TiO_2 particles was similar, the addition of different amount of OA might differentially influence particle aggregate states during the drying process. Therefore, the difference in coating surfaces of different OA: TiO_2 molar ratios might be attributed to particle size distribution and particle features of corresponding powders.

The specific CA and SA of different coatings are shown in Fig. 6. Overall, contact angles of TiO_2-OA coatings are close to the critical of 150°, and sliding angles are <5°. As for the sample with a ratio of 1:10, it shows a CA of 151.2°and a SA of 1.2°, a superhydrophobic performance. It indicates that full-surface coverage is necessary for a superb hydrophobic ability. As for nanocoatings, the combination of micro-scale nanoparticle aggregates and single nanoparticles on the aggregates provides a multi-scale roughness. This micro/nano hierarchical structure is

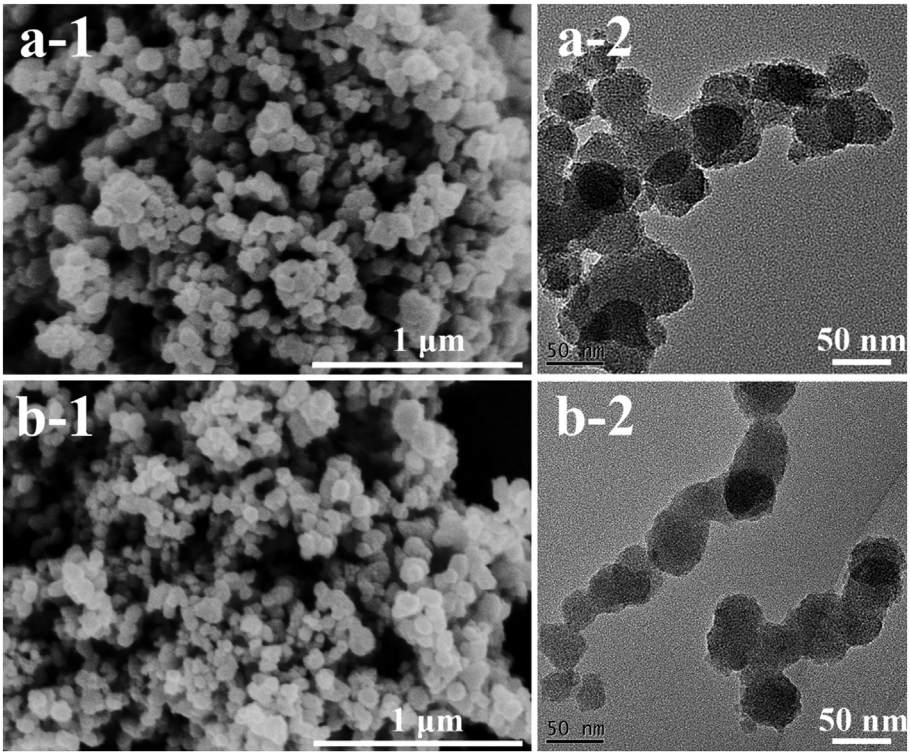

Fig. 2. FE-SEM (−1) and TEM (−2) images of (a) the starting TiO_2 nanoparticles and (b) the oleic acid (OA) treated TiO_2 nanoparticles.

rather conducive to the Cassie-Baxter state, which could be expressed by the equation:

$$\cos\theta^c = f_{SL}(\cos\theta_0 + 1) - 1$$

where θ_0 is the equilibrium CA on the plain surface, and θ^c is Cassie state CA, and f_{SL} is the fraction of liquid-solid contact. With a large number of nanometer-sized void spaces on the surface, a pretty low f_{SL} is supposed and thus a high θ^c But the exposure of hydrophilic parts will impair the non-wettability, causing the decrease of CA as well as the increase of SA, as indicated by coatings at a molar ratio of 1:1. Interestingly, the SA is still very low even if the CA was <150°. This excellent sliding property (i.e. having low SA but CA < 150°) were also observed in other nanocoatings [9,13].

The mechanical stability and the adhesive of the superhydrophobic coating deposited on aluminum with the dimension of 20 mm × 20 mm in length and width was assessed by scratch testing using 1500 grit Al_2O_3 sandpapers as the abrasion surface (Fig.7). Results show that the superhydrophobicity was maintained after abrasion tests, suggesting favorable mechanical stability and adhesive of the nanocoating on the substrate. The as-sprayed coating surface was a relatively smooth and compact layer with a number of submicrometer-sized clusters sparsely distributed on the top. After abrasion, nanoparticles underneath the surface were plowed out, exposing another fresh

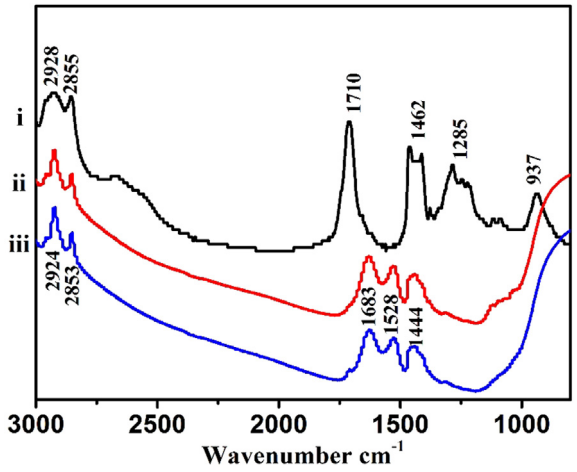

Fig. 3. FTIR spectra of (i) OA, (ii) TiO_2-OA powder and (iii) TiO_2-OA coating.

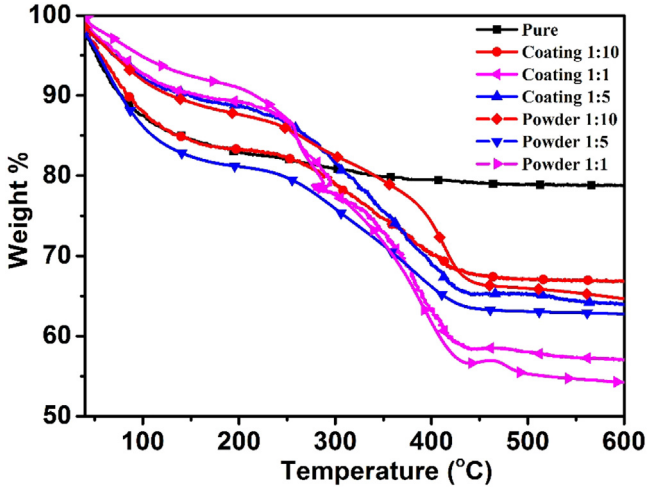

Fig. 4. TGA curves of TiO_2-OA powder and coatings with different molar ratios of OA to TiO_2.

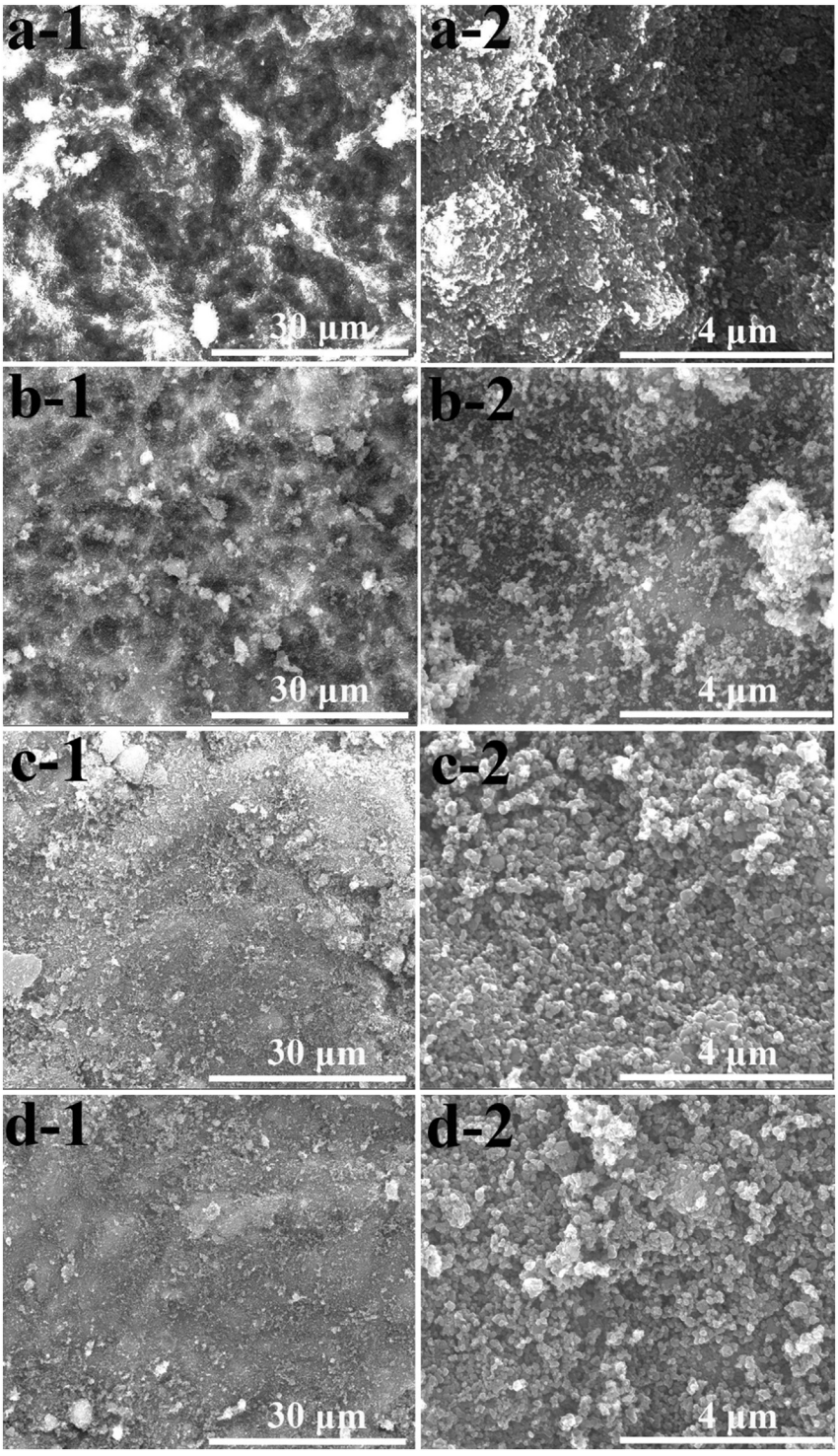

Fig. 5. FE-SEM images of the coatings fabricated by nanocomposites with different molar ratios of OA to TiO_2 in the starting TiO_2-OA powder, (a) pure TiO_2 (b) 1:1, (c) 1:5 and (d) 1:10 (−2 are enlarged views of selected areas in corresponding −1).

surface with a hierarchical structure (Fig. 7b). The surface roughness shows the Ra value of 3.4 μm and 4.4 μm for the coating before and after abrasion, respectively. Moreover, as the coating is composed of hydrophobic materials, no hydrophilic material would be exposed as long as the coating exists, which means that it could be regarded as a hydrophobic bulk material. This roughness-regenerating capability [32] and a hydrophobic bulk characteristic synergistically enable the coating to maintain superhydrophobicity after a certain degree of mechanical damage. This effect is illustrated schematically in Fig. 7e. It could be expected that other hydrophobic nanomaterials are also able to construct superhydrophobic nanocoatings through the VCS process.

4. Conclusion

We described a new way to fabricate superhydrophobic nanocoatings utilizing hydrophobic TiO_2 nanoparticles by a VCS process.

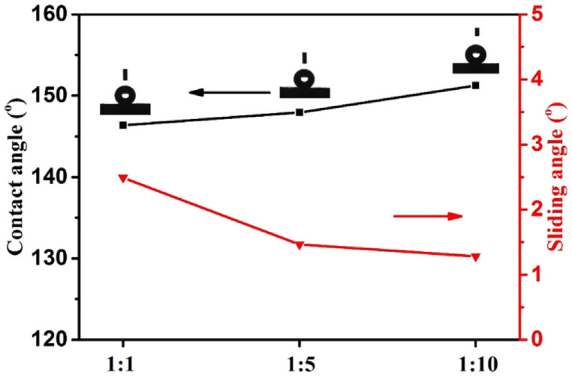

Fig. 6. Static water contact angles and sliding angles of the TiO_2-OA coatings with different molar ratios of OA to TiO_2 in the starting TiO_2-OA powder.

The wetting behavior of the as-sprayed coatings could be well tuned by adjusting the molar ratio of oleic acid to TiO_2. Water droplets could easily roll down from all the coating surfaces. With a molar ratio of 1:10 between oleic acid and TiO_2, a surface with a static water contact angle as high as 151.2° and a sliding angle as low as 1.2° was obtained. In particular, the newly constructed superhydrophobic nanocoatings could maintain their superhydrophobicity even after strong abrasion. The strategy adopted in this study might provide a new way to fabricate superhydrophobic nanocoatings using various nanoparticles modified with low surface energy materials.

Acknowledgments

This work was supported by National Natural Science Foundation of China (grant # 51401232), Ningbo Municipal Major Projects on Industrial Technology Innovation (grant # 2015B11054) and CAS-Iranian Vice Presidency for Science and Technology Joint Research Project (grant # 174433KYSB20160085).

Reference

[1] J. Genzer, K. Efimenko, Recent developments in superhydrophobic surfaces and their relevance to marine fouling: a review, Biofouling 22 (2006) 339–360.
[2] S.L. Zheng, C. Li, Q.T. Fu, W. Hu, T.F. Xiang, Q. Wang, M.P. Du, X.C. Liu, Z. Chen, Development of stable superhydrophobic coatings on aluminum surface for corrosion-resistant, self-cleaning, and anti-icing applications, Mater. Des. 93 (2016) 261–270.
[3] N. Wang, D.S. Xiong, Y.L. Deng, Y. Shi, K. Wang, Mechanically robust superhydrophobic steel surface with anti-icing, UV-durability, and corrosion resistance properties, ACS Appl. Mater. Interfaces 7 (2015) 6260–6272.
[4] J. Yang, Y.C. Tang, J.Q. Xu, B.B. Chen, H. Tang, C.S. Li, Durable superhydrophobic/superoleophilic epoxy/attapulgite nanocomposite coatings for oil/water separation, Surf. Coat. Technol. 272 (2015) 285–290.
[5] C. Lee, C.J. Kim, Underwater restoration and retention of gases on superhydrophobic surfaces for drag reduction, Phys. Rev. Lett. 106 (2011), 014502. .
[6] T.L. Sun, L. Feng, X.F. Gao, L. Jiang, Bioinspired surfaces with special wettability, Acc. Chem. Res. 38 (2005) 644–652.
[7] C.H. Xue, J.Z. Ma, Long-lived superhydrophobic surfaces, J. Mater. Chem. A 1 (2013) 4146–4161.
[8] Y.F. Si, Z.G. Guo, Superhydrophobic nanocoatings: from materials to fabrications and to applications, Nano 7 (2015) 5922–5946.
[9] D. Ebert, B. Bhushan, Transparent, superhydrophobic, and wear-resistant coatings on glass and polymer substrates using SiO_2, ZnO, and ITO nanoparticles, Langmuir 28 (2012) 11391–11399.
[10] Z.K. He, M. Ma, X.C. Xu, J.Y. Wang, F. Chen, H. Deng, K. Wang, Q. Zhang, Q. Fu, Fabrication of superhydrophobic coating via a facile and versatile method based on nanoparticle aggregates, Appl. Surf. Sci. 258 (2012) 2544–2550.
[11] Y. Ko, H. Baek, Y. Kim, M. Yoon, J. Cho, Hydrophobic nanoparticle-based nanocomposite films using in situ ligand exchange layer-by-layer assembly and their nonvolatile memory applications, ACS Nano 7 (2013) 143–153.
[12] J.B. Lin, H.L. Chen, T. Fei, J.L. Zhang, Highly transparent superhydrophobic organic-inorganic nanocoating from the aggregation of silica nanoparticles, Colloids Surf. A Physicochem. Eng. Asp. 421 (2013) 51–62.
[13] D. Kumar, X.H. Wu, Q.T. Fu, J.W.C. Ho, P.D. Kanhere, L. Li, Z. Chen, Hydrophobic sol-gel coatings based on polydimethylsiloxane for self-cleaning applications, Mater. Des. 86 (2015) 855–862.

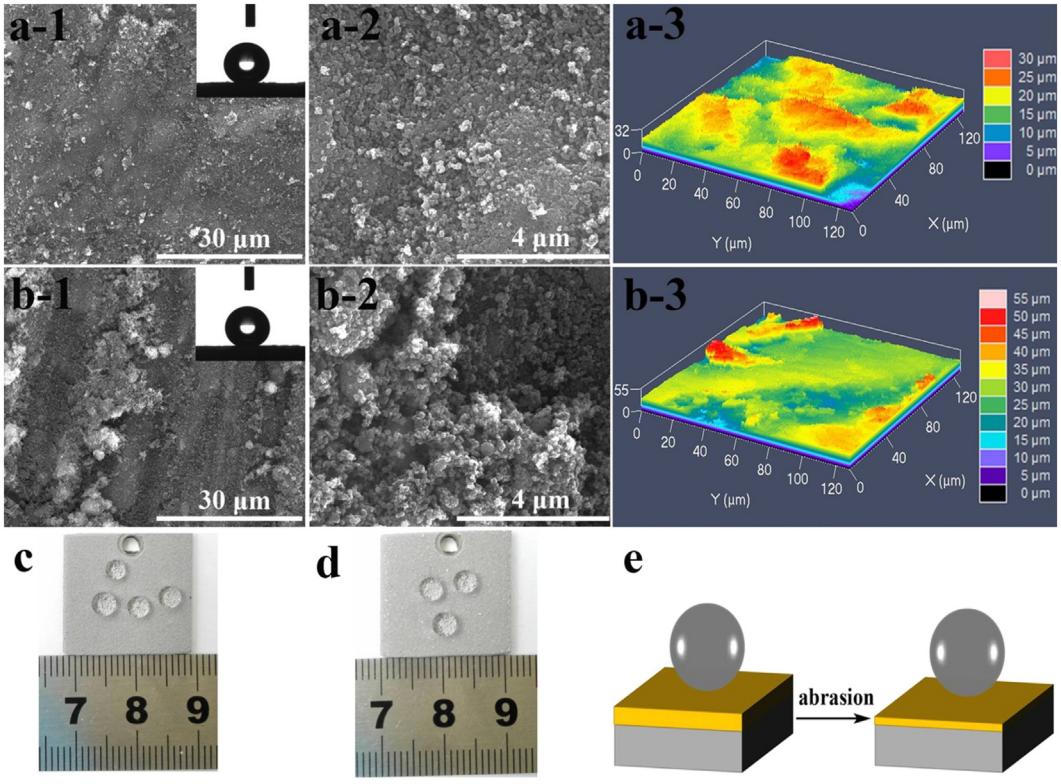

Fig. 7. FE-SEM and LSCM images of the superhydrophobic surface (a) before and (b) after abrasion (−2 are enlarged views of selected areas in corresponding −1, −3 are the surface profile of the coatings), digital image of water droplets standing on the superhydrophobic surface (20 mm × 20 mm) (c) before and (d) after abrasion, (e) schematic illustration shows that the superhydrophobic coatings made of hydrophobic nanocomposites will not introduce hydrophilic pinning sites and maintain superhydrophobicity after abrasion.

[14] D. Iacovetta, J. Tam, U. Erb, Synthesis, structure, and properties of superhydrophobic nickel-PTFE nanocomposite coatings made by electrodeposition, Surf. Coat. Technol. 279 (2015) 134–141.
[15] X.M. Bao, J.F. Cui, H.X. Sun, W.D. Liang, Z.Q. Zhu, J. An, B.P. Yang, P.Q. La, A. Li, Facile preparation of superhydrophobic surfaces based on metal oxide nanoparticles, Appl. Surf. Sci. 303 (2014) 473–480.
[16] D. Hong, I. Ryu, H. Kwon, J.J. Lee, S. Yim, Preparation of superhydrophobic, long-neck vase-like polymer surfaces, Phys. Chem. Chem. Phys. 15 (2013) 11862–11867.
[17] H. Ogihara, J. Xie, J. Okagaki, T. Saji, Simple method for preparing superhydrophobic paper: spray-deposited hydrophobic silica nanoparticle coatings exhibit high water-repellency and transparency, Langmuir 28 (2012) 4605–4608.
[18] W. Ming, D. Wu, R. van Benthem, G. de With, Superhydrophobic films from raspberry-like particles, Nano Lett. 5 (2005) 2298–2301.
[19] X.Y. Chen, J.H. Yuan, J. Huang, K. Ren, Y. Liu, S.Y. Lu, H. Li, Large-scale fabrication of superhydrophobic polyurethane/nano-Al_2O_3 coatings by suspension flame spraying for anti-corrosion applications, Appl. Surf. Sci. 311 (2014) 864–869.
[20] X.Y. Chen, Y.F. Gong, D.Y. Li, H. Li, Robust and easy-repairable superhydrophobic surfaces with multiple length-scale topography constructed by thermal spray route, Colloids Surf. A Physicochem. Eng. Asp. 492 (2016) 19–25.
[21] J. Akedo, Aerosol deposition of ceramic thick films at room temperature: densification mechanism of ceramic layers, J. Am. Ceram. Soc. 89 (2006) 1834–1839.
[22] S.Q. Fan, C.J. Li, C.X. Li, G.J. Liu, G.J. Yang, L.Z. Zhang, Preliminary study of performance of dye-sensitized solar cell of nano-TiO_2 coating deposited by vacuum cold spraying, Mater. Trans. 47 (2006) 1703–1709.
[23] K. Sahner, M. Kaspar, R. Moos, Assessment of the novel aerosol deposition method for room temperature preparation of metal oxide gas sensor films, Sensors Actuators B Chem. 139 (2009) 394–399.
[24] Y. Liu, J. Huang, H. Li, Nanostructural characteristics of vacuum cold-sprayed hydroxyapatite/graphene-nanosheet coatings for biomedical applications, J. Therm. Spray Technol. 23 (2014) 1149–1156.
[25] F. Su, K. Yao, Facile fabrication of superhydrophobic surface with excellent mechanical abrasion and corrosion resistance on copper substrate by a novel method, ACS Appl. Mater. Interfaces 6 (2014) 8762–8770.
[26] L. Yin, J. Yang, Y. Tang, L. Chen, C. Liu, H. Tang, C. Li, Mechanical durability of superhydrophobic and oleophobic copper meshes, Appl. Surf. Sci. 316 (2014) 259–263.
[27] X. Zhu, Z. Zhang, J. Yang, X. Xu, X. Men, X. Zhou, Facile fabrication of a superhydrophobic fabric with mechanical stability and easy-repairability, J. Colloid Interface Sci. 380 (2012) 182–186.
[28] X. Zhu, Z. Zhang, X. Men, J. Yang, K. Wang, X. Xu, X. Zhou, Q. Xue, Robust superhydrophobic surfaces with mechanical durability and easy repairability, J. Mater. Chem. 21 (2011) 15793–15797.
[29] C.C. Wang, J.Y. Ying, Sol-gel synthesis and hydrothermal processing of anatase and rutile titania nanocrystals, Chem. Mater. 11 (1999) 3113–3120.
[30] L. Zhang, R. He, H.C. Gu, Oleic acid coating on the monodisperse magnetite nanoparticles, Appl. Surf. Sci. 253 (2006) 2611–2617.
[31] P.D. Cozzoli, A. Kornowski, H. Weller, Low-temperature synthesis of soluble and processable organic-capped anatase TiO_2 nanorods, J. Am. Chem. Soc. 125 (2003) 14539–14548.
[32] T. Verho, C. Bower, P. Andrew, S. Franssila, O. Ikkala, R.H.A. Ras, Mechanically durable superhydrophobic surfaces, Adv. Mater. 23 (2011) 673–678.